Journal of Molecular Structure (Theochem), 281 (1993) 207–212
0166-1280/93/$06.00

Theoretical study on the methane activation reactions by Pt, Pt^+, and Pt^- atoms

M. Hada, H. Nakatsuji*, H. Nakai, S. Gyobu, S. Miki

Department of Synthetic Chemistry, Faculty of Engineering, Kyoto University, Kyoto 606, Japan

(Received 14 September 1992)

Abstract

The oxidative additions of CH_4 to the ground and excited states of Pt, Pt^-, and Pt^+ species are studied by the symmetry-adapted cluster (SAC) and SAC-CI methods. The reaction path is examined by calculating the Hellmann–Feynman forces acting on C and H atoms of CH_4. It involves the transition state and/or the activated complex. The activation energies of CH_4 with the triplet Pt(^{3}D; 5d9s1), singlet Pt(^{1}S; $5d^{10}$), anion Pt^-(^{2}S; $5d^{10}6s^1$), Pt^-(^{2}P; $5d^{10}6p^1$), and cation Pt^+(^{2}D; $5d^9$) are 102, 59, 75, 41, and 52 kcal mol^{-1} respectively. Further, there is a possibility for the excited state of the $Pt^- + CH_4$ system that the reaction proceeds with lower activation energy by relaxing onto the ground state curve along the reaction process. The activated complex $Pt^-(H)(CH_3)$ is 29 kcal mol^{-1} more stable than the dissociation limit of the excited $Pt^- + CH_4$ system. This suggests the possibility of C–H activation by photoexcited Pt^-. In the $Pt^-(H)(CH_3)$ complex, both bent and linear forms are possible; the two forms transform through an energy barrier of 22 kcal mol^{-1}. In the Pt and Pt^+ complexes, only the bent forms are stable.

Introduction

Activation of C–H bonds in saturated hydrocarbons is of wide significance for synthetic chemistry and industrial technology. Methane activation has been studied as one of the fundamental processes in these reactions. Possibilities of new catalytic processes for breaking C–H bonds via oxidative addition reactions have been studied, for example, by using naked metal atoms, metal complexes, metal clusters, and metal surfaces. There are many reports on the activation of methane by metal complexes [1]. For example, an Ir complex can break the C–H bond of methane as [2]

$$CH_4 + Ir(C_5Me_5)(PMe_3) \rightarrow IrH(CH_3)(C_5Me_5)(PMe_3)$$

* Corresponding author.

It has been reported that photoexcitation of metals assists the formation of the CH_3–M–H activated complexes for the metals Fe, Mn, Co, Zn, Ag, Au, and Ga [3,4]. The structures of the complexes have been shown to be linear for Cu and bent for Fe [4]. Further, the Al atom reacts with methane without photoexcitation [5,6].

Theoretical reports on the activation of methane with metals and metal complexes have recently appeared. The reaction mechanism in the elimination and addition reactions of methane for the Pt complex $Pt(H)(CH_3)(PH_3)_2$ has been studied by Morokuma and co-workers [7]. Reactions of CH_4 with Fe, Ni, and Pt clusters [8], and with naked Cu, Li, Mg, Ni, Pd, and Pt atoms [9–13] are also studied.

Theoretical studies of C–H activation in saturated hydrocarbons with charged and/or excited metals are necessary for analyses of experimental data and

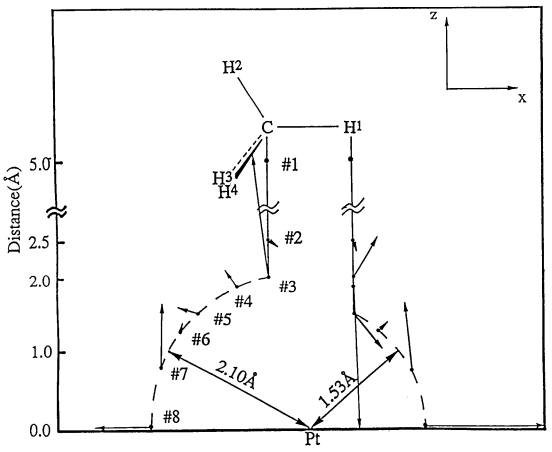

Fig. 1. The reaction path for the activation of the C–H bond in the Pt + CH_3 system, and the forces acting on the C and H atoms calculated from the Hartree–Fock wavefunctions.

designing reactions. The reactivities of the neutral and charged metals and those of the ground and excited states are expected to be quite different. For example, the excited Cr^+ (^6S) atom activates only the C–C bond, whereas the Cr^+ (^4D, ^4G) atom activates both C–C and C–H bonds of hydrocarbons [14]. In this report, the oxidative additions of methane by the ground and excited states of the neutral Pt atom, Pt anion, and Pt cation are studied by the ab initio Hartree–Fock and the symmetry-adapted cluster (SAC) and SAC-CI methods [15].

Method of calculation

The gaussian basis set of double-zeta accuracy ((3s2p5d)/[3s2p3d]) is used for the valence electrons of the Pt atom and the core electrons are replaced by the effective core potential of Hay and Wadt [16]. 4-31G Basis sets [17] are used for C and H atoms. In order to calculate accurate Hellmann–Feynman forces acting on C and H atoms, the derivative AOs of the 4-31G set are added to the basis sets for C and H atoms [18].

The reaction path for the Pt + CH_4 system is shown in Fig. 1. This is based on the preliminary global calculations for the system and is fixed throughout the present calculations. The Pt atom of the reaction system is located at the bottom of Fig. 1. The assumptions for constructing the reaction path are as follows. When the distance between Pt and CH_4 is large (# 1–# 2), the preferable form for CH_4 is side-on as the Pt atom is inserted into one of the C–H bonds. After CH_4 comes to # 3, the CH_3 group moves along the circle whose radius is 2.10 Å, while the H1 atom approaches the Pt atom continuously (# 3–# 5). The radius 2.10 Å is the Pt–C distance of the Pt(CH_3) molecule optimized by Hartree–Fock calculations. When CH_4 come to # 5, the H1 atom also starts to move along the other circle whose radius is 1.53 Å; this radius is the experimental Pt–H distance of the diatomic PtH molecule [19]. The C–H bond is elongated gradually from # 3, while the structure of the CH_3 group is fixed to that of CH_4. The CH_3 group is oriented toward the H1 atom in # 3 and # 4, then it inclines toward the Pt atom after # 4.

First, we examine the reaction path described above by using the Hellmann–Feynman forces acting on the C and H atoms in the Pt + CH_4 system. The forces are obtained from the closed shell Hartree–Fock wavefunctions. Then, using the reaction path, the potential curves for the ground and excited states of the neutral, electron-attached and cationic systems Pt + CH_4, Pt^- + CH_4 and Pt^+ + CH_4, respectively, are calculated by the SAC and SAC-CI methods. In these methods, one 1s orbital of the C atom is frozen and the 36 orbitals are included in the active orbitals. The programs used in this calculation are HONDO 7 [20] for Hartree–Fock and SAC 85 [21] for SAC and SAC-CI methods.

Results and discussion

Reaction path

The reaction path defined in the previous section and the forces acting on the C and H1 atoms in CH_4 are shown in Fig. 1. These forces are calculated from the Hartree–Fock wavefunctions. The ground state is always a closed-shell singlet throughout the reaction path except near the dissociation limit

(# 1), so we can examine the reaction path by use of these forces. Details on the ground and excited states will be discussed in the next section (Neutral systems). At # 1, no appreciable forces act on C and H atoms, indicating that there is no interaction between Pt and CH_4. At # 2, the attractive forces towards the Pt atom acting on both C and H atoms increase gradually. At # 3, large repulsive forces appear on both C and H atoms, suggesting that the transition state of the Pt–CH_4 complex exists between # 2 and # 3, and that there is a potential barrier around # 3. At # 4 and # 5, forces acting on H are strongly attractive to Pt, while forces acting on C are slightly repulsive. This suggests that the interaction between H and Pt may be important when CH_4 approaches Pt in the first stage of the reaction. The forces acting on C and H almost disappear at # 6. The stable complex is formed at # 6, in which the C–H bond is completely cleaved. The optimized H–Pt–C bond angle of the activated complex around # 6 is 87°, which agrees with the other theoretical results (91°) [13]. Large repulsive forces appear around # 7.

We have confirmed that the reaction path shown in Fig. 1 includes the activated complex and there is the potential barrier around # 3 before the activated complex appears. We suppose that the methane activation reaction proceeds approximately along the reaction path shown in Fig. 1. All the calculations for the C–H activation reactions by the ground and excited Pt, Pt^-, and Pt^+ species are carried out using the same reaction path examined above for the ground Pt + CH_4 system.

Neutral systems

Figures 2 and 3 show the potential curves of the neutral reaction system in the triplet and singlet states respectively. The reaction path is defined in Fig. 1. At the dissociation limit (# 1) the ground state of the system is triplet, because the ground state of the Pt atom is $^3D(d^9s^1)$: the calculated singlet–triplet energy separation is 12 kcal mol^{-1} in comparison with the experimental value for the Pt atom of 17.6 kcal mol^{-1} [22]. The potential curves

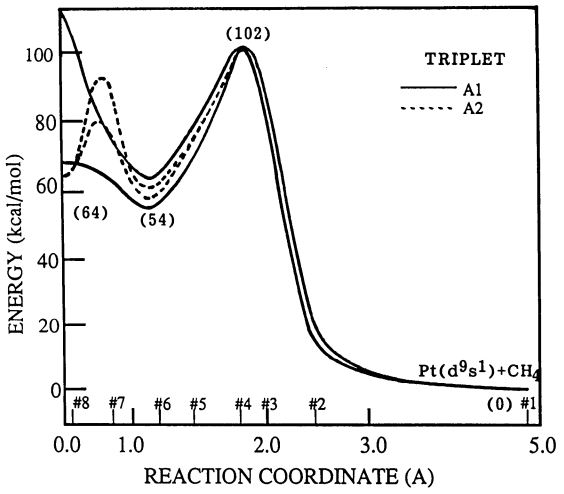

Fig. 2. Low lying triplet potential curves for the activation of the C–H bond with Pt along the reaction path shown in Fig. 1. The calculations are by the SAC and SAC-CI methods and the values in parentheses are the energies in kcal mol^{-1} relative to the initial Pt(^{3}D) + CH_4 system.

before # 2 are flat and slightly repulsive. After # 2, the potential curve for the first singlet state becomes the lowest one in Figs. 2 and 3: this state has the Hartree–Fock configuration as a main component. The transition states appear around # 3–# 4. The

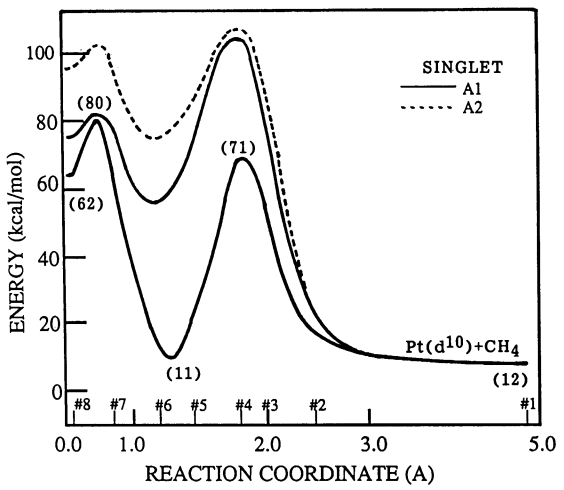

Fig. 3. Low lying singlet potential curves for the activation of the C–H bond with Pt along the reaction path shown in Fig. 1. The calculations are by the SAC and SAC-CI methods and the values in parentheses are the energies in kcal mol^{-1} relative to the initial Pt(^{1}S) + CH_4 system.

energy barriers for the activation of the C–H bond are 102 and 59 kcal mol^{-1} for the triplet and singlet reaction systems respectively. The H–Pt–CH_3 activated complex, in which one of the C–H bonds is completely cleaved, are formed at #6 in the first singlet state. It is slightly more stable than the Pt(^{1}S; d^{10}) + CH_4 system, although it is 11 kcal mol^{-1} more unstable than the Pt(^{3}D; d^9s^1) + CH_4 system. The activated complex in the triplet state is 54 kcal mol^{-1} higher in energy than the Pt(^{3}D; d^9s^1) + CH_4 system. The linear complexes can also exist at #8 for the singlet state, though they are more unstable.

The singlet and triplet potential curves in Figs. 2 and 3 have a crossing around #2. Considering the spin–orbit coupling of this system, the triplet Pt atom can activate the C–H bond of CH_4 with an activation energy of 71 kcal mol^{-1}. However, this activation energy is larger than that of the singlet Pt + CH_4 system.

The singlet ground state seems to be the probable state in the C–H activation reaction, so we focus on its electronic structure. The electronic configuration of Pt is d^{10} at #1–#2, d^9s^1 at #3–#7, and $d^8s^1p^1$ at #8. Before #2, there is no interaction between the excited state Pt(d^{10}) atom and CH_4. After #2, the Pt–C and Pt–H bonding orbitals are gradually formed by the donation of electrons from the C–H bonding orbital to the unoccupied s orbital of Pt, and by the back donation from the d_{xz} orbital of Pt to the C–H antibonding orbital. In the activated complex (#6), the Pt–H and Pt–C bonding orbitals are completely formed by the $6s5d_{xz}$ hybrid orbitals and the configuration Pt(d^{10}) is transformed to Pt(d^9s^1). This bond character is also understood from the stable geometry of the activated complex. We note that the bond character is the same as in the Pd–H_2 complex [23], although the H–H bond is not cleaved in the Pd–H_2 system. The linear complex at #8 is 51 kcal mol^{-1} higher in energy. The Pt–C and Pt–H bonds are formed by the $6p5d_{xx}$ hybrid orbitals, and the electronic structure of Pt becomes d^9p^1. Replacing the doubly occupied 2sp(C)–$5d_{xy}$(Pt)–1s(H) orbital with the 2sp(C)–$6p_x$(Pt)–1s(H) orbital is necessary for forming the linear complex after #7, causing the potential barrier around #7–#8.

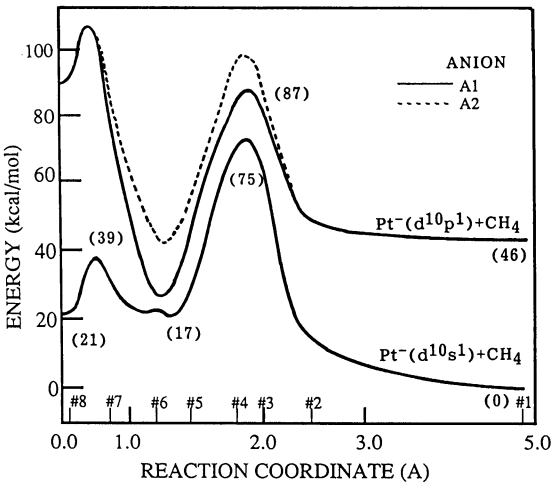

Fig. 4. Low lying potential curves for the activation of the C–H bond with the Pt anion along the reaction path shown in Fig. 1. The calculations are by the SAC and SAC-CI methods and the values in parentheses are the energies in kcal mol^{-1} relative to the initial Pt$^-$(^{2}S) + CH_4 system.

Charged systems

Figures 4 and 5 show the potential curves for the doublet states of the electron-attached system Pt^- + CH_4 and the cationic system Pt^+ + CH_4 respectively. We first study the reactivity of the Pt anion. At #1, the energy separation between the $d^{10}s^1$ and $d^{10}p^1$ configurations of Pt^- is 43 kcal mol^{-1}. In Fig. 4, the ground state is $^2A_1$ throughout the reaction path and dissociates into Pt($d^{10}s^1$) + CH_4. Total energies for the transition state and the activated complex are 75 and 17 kcal mol^{-1}, respectively, compared with that of the dissociation limit. These are higher than those of the neutral singlet system, because the electron donation from the C–H bond to the half-occupied 6s orbital of Pt is more difficult than the donation to the vacant 6s orbital. Relative to the energy of Pt$^-$($d^{10}p^1$) + CH_4, the transition state and activated complex are 32 and −26 kcal mol^{-1}, respectively, suggesting the possibility that the excited Pt anion may activate the C–H bond of CH_4 with a smaller activation

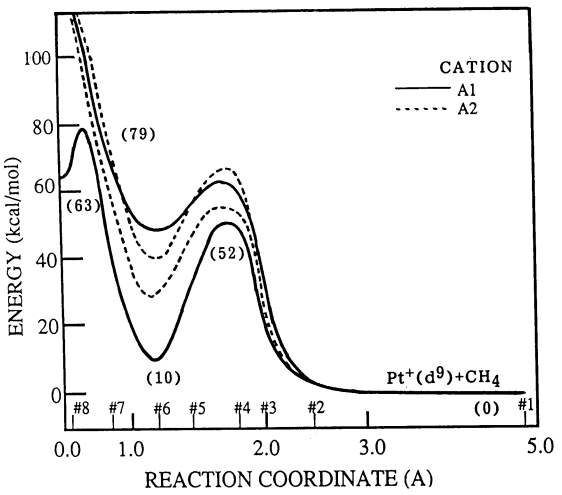

Fig. 5. Low lying potential curves for the activation of the C–H bond with the Pt cation along the reaction path shown in Fig. 1. The calculations are by the SAC and SAC-CI methods and the values in parentheses are the energies in kcal mol^{-1} relative to the initial $Pt^+(^2D) + CH_4$ system.

energy (approximately 32 kcal mol^{-1}), after a transition to the ground state around #2–#3.

Two potential curves for the anion state are close to each other around #6; the avoided crossing of the electronic configuration occurs around here. Before and after #6, the electronic structures of Pt in the ground state are $d^{10}s^1$ and $d^{10}p^1$ respectively. The relaxation from the upper to the lower states occurs easily around here. The linear complex at #8 is also as stable as the bent complex at #6 in the ground state. The energy barrier between the two complexes at #6 and #8 is 22 kcal mol^{-1}, which is lower than that in the neutral system, so the complex may change the geometry from bent to linear. The lowering of the potential barrier around #7–#8 is due to the fact that the 6p orbital of $Pt^-(d^{10}p^1)$ is already half-occupied in the ground state after the avoided crossing around #6. Only one-electron flow into p orbital is required to change the form, whereas in the neutral system two-electron flow is required.

We next investigate the cationic system $Pt^+ + CH_4$. From Fig. 5, we see that the transition state and the activated complex are respectively 52 and 10 kcal mol^{-1} higher than the separated system. The energy barrier of the reaction is smaller than that of the reaction of the neutral Pt atom. The linear form is 53 kcal mol^{-1} less stable than the bent form in the activated complex. The $5d_{z^2}$ and 6s orbitals of Pt play the same role as that of the 6s orbital in the neutral system. As a whole, the shape of the potential curve for the cation ground state is similar to that for the neutral singlet ground state.

Summary

The oxidative addition reactions of the ground and excited states of the neutral Pt atom, Pt^- anion, and Pt^+ cation to the C–H bond of CH_4 have been studied by the Hartree–Fock, the SAC and SAC-CI methods. The following is a summary of the present study.

(1) The reaction path assumed in this report has been examined by the Hellmann–Feynman forces acting on C and H atoms in CH_4. This reaction path includes the transition state and the activated complex.

(2) The excited state of the $Pt^-(d^{10}p^1)$ anion can activate the C–H bond of CH_4 with the smallest activation energy of 41 kcal mol^{-1}. The $Pt^+(d^9)$ cation and singlet excited $Pt(d^{10})$ atom can also activate the C–H bond with activation energies of 52 and 59 kcal mol^{-1} respectively.

(3) The reaction with the lowest activation energy is suggested for the excited $Pt^- + CH_4$ system. This reaction may occur after photolysis of the charged metal.

(4) The neutral triplet $Pt(d^9s^1)$ and the ground $Pt^-(d^{10}s^1)$ anion activate the C–H bond of CH_4 with much higher potential barriers of 102 and 75 kcal mol^{-1} respectively.

(5) The linear form is as stable as the bent form for the anion complex $Pt^-(H)(CH_3)$: the potential barrier is 22 kcal mol^{-1}.

References

1 D. R. Alexander, Chem. Rev., 90 (1990) 403.
2 A. H. Janowicz and R. G. Bergman, J. Am. Chem. Soc., 104 (1982) 352.

3 W. E. Billups, M. M. Kararski, H. R. Hauge and J. L. Margrave, J. Am. Chem. Soc., 102 (1982) 7393.
4 (a) G. A. Ozin and F. M. Douglas, J. Am. Chem. Soc., 103 (1981) 1574.
(b) G. A. Ozin and J. G. McCaffrey, J. Am. Chem. Soc., 104 (1982) 7351.
5 K. J. Klabunde and Y. Tanaka, J. Am. Chem. Soc., 105 (1983) 3544.
6 D. G. Leopold, J. Ho and W. C. Lineberger, J. Chem. Phys., 86 (1987) 1715.
7 S. Obara, K. Kitaura and K. Morokuma, J. Am. Chem. Soc., 106 (1984) 7482.
8 A. B. Anderson and J. J. Malonely, J. Phys. Chem., 92 (1988) 809.
9 S. Castillo, E. Poulain and O. Novaro, Int. J. Quantum Chem. Symp., 23 (1989) 509.
10 J. G. McCaffrey, R. A. Poirier, G. A. Ozin and I. G. Csizmadia, J. Am. Chem. Soc., 88 (1984) 2898.
11 P. Chaquin, A. Papakondylis, C. Giessner-Prettre and A. Sevin, J. Phys. Chem., 94 (1990) 7352.
12 M. R. A. Blomberg, Ulf Brandemark and P. E. M. Siegbahn, J. Am. Chem. Soc., 105 (1983) 5557.
13 J. J. Low and A. Goddard, Organometallic, 5 (1986) 610.
14 E. R. Fisher and P. B. Armentrout, J. Am. Chem. Soc., 114 (1992) 2049.
15 (a) H. Nakatsuji and K. Hirao, J. Chem. Phys., 68 (1978) 2035.
(b) H. Nakatsuji, Chem. Phys. Lett., 59 (1978) 362; 67 (1979) 329.
(c) H. Nakatsuji, Chem. Phys., 75 (1983) 425.
16 P. J. Hay and W. R. Wadt, J. Chem. Phys., 82 (1985) 270.
17 R. Ditchfield, W. J. Hehre and J. A. Pople, J. Chem. Phys., 54 (1971) 724.
18 (a) H. Nakatsuji, K. Kanda and T. Yonezawa, Chem. Phys. Lett., 75 (1980) 340.
(b) H. Nakatsuji, K. Kanda, M. Hada and T. Yonezawa, J. Chem. Phys., 77 (1982) 3109.
19 K. P. Huber and G. Herzberg, Molecular Spectra and Molecular Structures. IV. Constants of Diatomic Molecules, Van Nostrand, Princeton, 1974.
20 M. S. Dupuis, J. D. Watts, H. O. Villar and G. J. B. Hurst, HONDO 7, IBM, Scientific and Engineering Computations, Dept. 48B, New York, 1978.
21 H. Nakatsuji, Program System for SAC and SAC-CI Calculations, Program Library No. 146 (Y4/SAC), Data Processing Center of Kyoto University, 1985; Program Library SAC85, No. 1396, Computer Center of Institute for Molecular Science, Okazaki, Japan, 1986.
22 C. E. Moore, Natl. Bur. Stand. (U.S.), Circ., 467(1) (1958).
23 H. Nakatsuji, M. Hada and T. Yonezawa, J. Am. Chem. Soc., 109 (1987) 1902.